Proceedings of the
International Conference on Mechanical Engineering 2011
(ICME2011) 18-20 December 2011, Dhaka, Bangladesh

ICME11-FL-012

NON-ISOTHERMAL FLOW THROUGH A ROTATING STRAIGHT DUCT WITH RECTANGULAR CROSS-SECTION

Mohammad Wahiduzzaman and Md. Mahmud Alam
Mathematics Discipline, Khulna University, Khulna, Bangladesh

ABSTRACT

The incompressible viscous steady Non-isothermal fluid flow through a straight duct of rectangular cross-section rotating at a constant angular velocity about the center of the duct cross-section is investigated numerically to examine the combined effects of Rotation parameter (Coriolis force), Grashof number, Prandtl number, aspect ratio and Pressure-driven parameter (centrifugal force) on the flow. Spectral method is applied as a main tool for the numerical technique, where the Chebyshev polynomial, the Collocation methods, the Newton-Raphson method, the Are-length method are also used as secondary tools. The flow structures are examined in case of Rotation of the duct axis and the Pressure-driven parameter with large aspect ratio where other parameters are fixed. The calculations are carried out for $0 \leq T_r \leq 150, \gamma \leq 6, G_r = 100, P_r = 7.0$ and $0 \leq P_{gr} \leq 800$ by applying the Spectral method. When $\Omega > 0$ and the rotation is in the same direction as the Coriolis force enforces the centrifugal force, multiple solutions of Non-symmetric secondary flow patterns with 6-vortex (maximum) are obtained in case of $P_{gr} = 500$ and 800 with large aspect ratio, while the centrifugal force enforces coriolis force, multiple solutions of Non-symmetric the secondary flow patterns with 10-vortex (maximum) are obtained in case of $T_r = 100$ and 150 with large aspect ratio.

Keywords: Aspect Ratio, Dean Number, Rotation Parameter

1. INTRODUCTION

When a straight duct rotates at a constant angular velocity about the axis of its cylindrical symmetry, the flowing of fluid in the straight duct is subjected to both a Coriolis and a centrifugal forces. Such a rotating passages are used in cooling system for conductors of electric generators and generator motors for pumped-storage stations. The earliest work on this subject focused on theoretical investigations of laminar flow in a 'weakly rotating' circular pipe. To the best of the author's knowledge, most of the previous works on flow through a rotating straight ducts have been performed on a qualitative basis. Yang *et. al*. (1994) reviewed in detail the literature on rotating duct flow. For this kind of flow, Ito and Nanbu (1971) and Ito (1959) derived dimensionless parameters using integral method. Ishigaki (1994) introduced the dimensionless parameters to demonstrate the quantitative analogy of flows in a circular pipe and obtained satisfactory results. Lee and Baek (2001), confirmed the quantitative analogy of fully developed laminar flow in orthogonally rotating straight duct and stationary curved ducts of square cross-section, using dimensionless parameters suggested by Ishigaki (1994). Lee and Baek (2002) showed the similarity of fully developed laminar flows in orthogonally rotating straight rectangular duct and stationary curved rectangular duct of arbitrary aspect ratio.

Our aim is to study the Non-isothermal fluid flow through a rotating straight duct with rectangular cross-section, where the outer wall of the duct cross-section is heated and inner wall is cooled. Studying the effect of rotation, pressure driven parameter, Grashof number, Prandtl number and large aspect ratio on the flow characteristic as well as solution structure are an important object of this paper. Numerical solutions are obtained by the Spectral method as a main tool and Newton-Raphson method, collocation method and are-length method are used as a secondary tools.

2. GOVERNING EQUATION

We shall consider the fully developed flow through a straight duct with rectangular cross-section. Let $2l$ is the width of the duct cross-section and $2h$ its height. Figure 1 shows the Cartesian co-ordinate system (x', y', z') and the same co-ordinate also (x', y', z') with the center C in a cross-section of the straight duct. The system rotates at a constant angular velocity, $\Omega = (0, -\Omega, 0)$ around the $y-$axis. The flow is drive by pressure gradient $-\frac{\partial p'}{\partial z'} = c_1'$ along the central line of the duct. i.e, the main (axial) flow is in the $z'-$direction as shown in Figure 1.
Thus, introducing the following non-dimensional quantities as follows:

$$u' = \frac{\nu}{l}u, v' = \frac{\nu}{l}v, w' = \frac{\nu}{l}w, x' = lx, y' = ly, p' = \frac{\rho\nu p}{l^2}$$
$$T' = (\Delta T)T$$

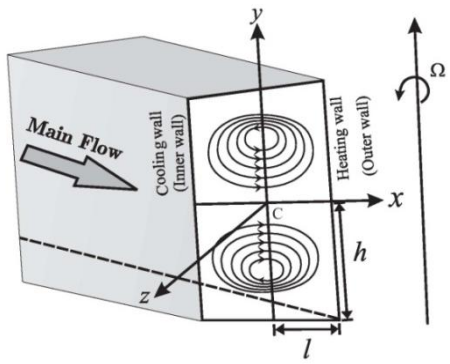

Fig 1. Rotating straight duct.

where, l is the half width of the duct cross-sectional, ν is the kinematic viscosity. k is the thermal conductivity, g is the acceleration due to gravity, u', v', w' is the dimensional velocity components along x', y', z' direction respectively, u, v, w is the dimensionless velocity components along x, y, z direction respectively, p' is the modified pressure, t is the time, T' is the temperature of the flow field, T is the dimensionless temperature of the flow field.

The non-dimensional continuity, momentum and energy equations of the problem are:

$$\frac{\partial u}{\partial x}+\frac{\partial u}{\partial y}=0 \quad (1)$$

$$u\frac{\partial u}{\partial x}+v\frac{\partial u}{\partial y}=-\frac{\partial p}{\partial x}+\frac{\partial^2 u}{\partial x^2}+\frac{\partial^2 u}{\partial y^2}+T_r w \quad (2)$$

$$u\frac{\partial v}{\partial x}+v\frac{\partial v}{\partial y}=-\frac{\partial p}{\partial y}+\frac{\partial^2 v}{\partial x^2}+\frac{\partial^2 v}{\partial y^2}+G_r \quad (3)$$

$$u\frac{\partial w}{\partial x}+v\frac{\partial w}{\partial y}=p_{gr}+\frac{\partial^2 w}{\partial x^2}+\frac{\partial^2 w}{\partial y^2}-T_r u \quad (4)$$

$$u\frac{\partial T}{\partial x}+v\frac{\partial T}{\partial y}=\frac{1}{p_r}\left(\frac{\partial^2 T}{\partial x^2}+\frac{\partial^2 T}{\partial y^2}\right) \quad (5)$$

where, $\tilde{p}=p'+\rho g y$, $T_r=\frac{2l^2\Omega}{\nu}$ (Rotational parameter), $p_{gr}=\frac{l^3}{\nu\rho}c_1'$ (Pressure driven parameter), $G_r=\frac{g\beta l^{3(\Delta T)}}{\nu^2}$(Grashof number) and $p_r=\frac{\nu}{\frac{k}{\rho c_p}}$ (Prandtl number).

The boundary conditions are that the velocities are zero at $x=\pm 1, y=\pm 1$.

Since the flow is uniform in the $z-$direction the sectional stream function $\psi(x,y)$ is introduced in the x and y direction as follows:

$$u=\frac{\partial\psi}{\partial y}, v=-\frac{\partial\psi}{\partial x} \quad (6)$$

which satisfies the continuity equation (1).

We introduce a new variable $\bar{y}$ in the y direction as $y=\gamma\bar{y}$, where, $\gamma=\frac{h}{l}$ is the aspect ratio h and l are the half height and width of the duct cross-section respectively.

Using equation (6) and other variables, the equations (1) - (5) become,

$$\frac{1}{\gamma^3}\frac{\partial\psi}{\partial\bar{y}}\frac{\partial^3\psi}{\partial x\partial\bar{y}^2}-\frac{1}{\gamma}\frac{\partial\psi}{\partial x}\frac{\partial^3\psi}{\partial x^2\partial\bar{y}}+\frac{1}{\gamma}\frac{\partial\psi}{\partial\bar{y}}\frac{\partial^3\psi}{\partial x^3}-\frac{1}{\gamma^3}\frac{\partial\psi}{\partial x}\frac{\partial^3\psi}{\partial\bar{y}^3}=\frac{\partial^4\psi}{\partial x^4}+\frac{2}{\gamma}\frac{\partial^4\psi}{\partial x^2\partial\bar{y}^2}+\frac{1}{\gamma^4}\frac{\partial^4\psi}{\partial\bar{y}^4}+\frac{T_r}{\gamma}\frac{\partial w}{\partial\bar{y}}-G_r\frac{\partial T}{\partial x} \quad (7)$$

$$\frac{1}{\gamma}\frac{\partial\psi}{\partial\bar{y}}\frac{\partial w}{\partial x}-\frac{1}{\gamma}\frac{\partial\psi}{\partial x}\frac{\partial w}{\partial\bar{y}}=p_{gr}+\frac{\partial^2 w}{\partial x^2}+\frac{1}{\gamma^2}-\frac{T_r}{\gamma}\frac{\partial\psi}{\partial\bar{y}} \quad (8)$$

$$\frac{1}{\gamma}\frac{\partial\psi}{\partial\bar{y}}\frac{\partial T}{\partial x}-\frac{1}{\gamma}\frac{\partial\psi}{\partial x}\frac{\partial T}{\partial\bar{y}}=\frac{1}{p_r}\left(\frac{\partial^2 T}{\partial x^2}+\frac{1}{\gamma^2}\frac{\partial^2 T}{\partial\bar{y}^2}\right) \quad (9)$$

The equations for ψ, w and T are actually used for numerical calculation. The boundary conditions for ψ, w and T are given by

$w(\pm 1,\bar{y})=w(x,\pm 1)=\psi(\pm 1,\bar{y})=\psi(x,\pm 1)=\frac{\partial\psi}{\partial x}(\pm 1,\bar{y})=\psi(x,\pm 1)=\frac{\partial\psi}{\partial\bar{y}}(x,\pm 1)=0$

and the temperature is assumed to be constant on the wall as

$T(\pm 1,\bar{y})=\pm 1, T(x,\pm 1)=x$ (heating outer wall)

$T(\mp 1,\bar{y})=\mp 1, T(x,\mp 1)=-x$ (cooling inner wall)

The case of heating the outer side wall and cooling the inner side wall can be deduced directly from the results obtained in this study.

The Total Flow Through the Duct

The dimensional total flow Q' through the duct is calculated by

$$Q'=\int_{-h}^{h}\int_{-l}^{l} w\,dx'dy'=\nu\, l\, Q$$

where, $Q=\int_{-\gamma}^{\gamma}\int_{-1}^{1} w\,dxd\bar{y}$ is the dimensionless total flow.

3. METHOD OF NUMERICAL CALCULATION

The method adopted in the present numerical calculation is Spectral method. The series of the Chebyshev polynomial is used in the x and y directions where x and y are the variables. Assuming the flow is symmetric along the horizontal line. The expansion function $\Phi_n(x)$ and $\Psi_n(x)$ are expressed as:

$\Phi_n(x)=(1-x^2)C_n(x)$, $\Psi_n(x)=(1-x)^2C_n(x)$ (19)

where, $C_n(x)=cos(ncos^{-1}(x))$ is the $n-$th order Chebyshev polynomial. $w(x,y,t)$, $\psi(x,y,t)$ and $T(x,y,t)$ are expanded in terms of the function $\Phi_n(x)$ and $\Psi_n(x)$ as:

$$w(x,y,t)=\sum_{m=0}^{M}\sum_{n=0}^{N} w_{mn}(t)\,\Phi_m(x)\Phi_n(y) \quad (20)$$

$$\psi(x,y,t)=\sum_{m=0}^{M}\sum_{n=0}^{N} \psi_{mn}(t)\,\Psi_m(x)\Psi_n(y) \quad (21)$$

$$T(x,y,t)=\sum_{m=0}^{M}\sum_{n=0}^{N} T_{mn}(t)\,\Phi_m(x)\Phi_n(y)+x \quad (22)$$

where M, N are the truncation numbers in the x and y directions respectively, and w_{mn} , ψ_{mn} and T_{mn} are the coefficients of expansion. In order to obtain the solutions for $w(x,y,t)$, $\psi(x,y,t)$ and $T(x,y,t)$, the expansion series (20)-(22) are substituted into the basic equations (16)-(18). The collocation method (Gottlieb and Orszag,1977) applied in x and y directions yield a set of nonlinear differential equations for w_{mn} , ψ_{mn} and T_{mn} . The collocation points x_i, y_i are taken as:

$$x_i=cos\left[\pi\left(1-\frac{i}{M+2}\right)\right],\quad (i=1,\ldots\ldots M+1) \quad (23)$$

$$y_i=cos\left[\pi\left(1-\frac{j}{N+2}\right)\right],\quad (i=1,\ldots\ldots N+1) \quad (24)$$

The obtained numerical algebraic equations are solved by Newton-Raphson method as well as Arc-length method. The convergence is assured by taking sufficiently small $\epsilon_p(\epsilon_p<10^{-8})$ defined as:

$$\epsilon_p = \sum_{m=0}^{M}\sum_{n=0}^{N} [(w_{mn}^{(p+1)} - w_{mn}^{(p)})^2 + (\psi_{mn}^{(p+1)} - \psi_{mn}^{(p)})^2 + (T_{mn}^{(p+1)} - T_{mn}^{(p)})^2] \quad (25)$$

For sufficient accuracy of the solution, we take $M = 16$ and $N = 32$ for the rectangular duct cross-section.

4. RESULTS AND DISCUSSION

Steady solution for Non-Isothermal flow (Grashof number $G_r = 100$):

We take the convective rotating straight duct having different aspect ratio (γ) to investigate the flow characteristics with pressure deriven parameter (P_{gr}), rotation parameter (T_r) and prandtl number $P_r = 7.0$, for water) effect.The numerical calculations are carried out for water at an external heat on the outer wall of the duct. We investigate the flow characteristics with varying pressure deriven parameter while rotational parameter remains constant and vice versa. For the above mentioned purposes, we consider two cases, *Case* I: $\gamma = 6$ and $P_{gr} = 500$ and *Case* II: $\gamma = 6$ and $p_{gr} = 800$. Thus an interesting and complicated flow behaviour of the above mentioned two cases will be expected, if the duct rotation is involved in these convective cases. According to the definition of T_r means that the rotational direction is in the same as that of main flow. First, the accuracy of the numerical calculation is investigated for the truncation numbers M and N are used in this investigation. For a good accuracy of the solutions, N is chosen equal to γM, where, γ is the aspect ratio of the duct cross section. After a detail investigation over the truncation numbers, it is concluded that the values $M = 16$ and $N = 32$ give sufficient accuracy for the present numerical calculations, the details are not given here for brevity.

Case I: $\gamma = 6$ and $p_{gr} = 500$

The steady solution curve is obtained for $\gamma = 6$ and $p_{gr} = 500$ in the range $0 \le T_r \le 70$ and the Figure 2 shows the steady solution curve. Figure 2 shows the total flow Q through the duct versus the Rotational parameter T_r. The complicated region of the solution curve are enlarged to understand clearly. We found that steady solution curve consists of 15 sections. These 15 sections of the solution curve are shown in enlargement shape in Figures 3(a)-3(d). The solution curve starts with the curve r_1 (Figure 3(a)) initially with $T_r = 15$ and turns at a point, where $T_r = 70$. The other section curves are represented by $r_2 - r_{15}$ (see Figures 3(a)-3(d)).

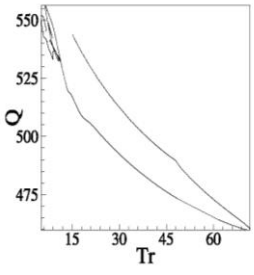

Fig 2. Steady solution curve for $\gamma = 6$, $p_{gr} = 500$, $P_r = 7.0, G_r = 100$ and $0 \le T_r \le 70$.

We now discuss the variation of the secondary flow, the axial flow and the temperature field at several values of T_r on the solution curve for constant ψ, w and T. We look the figures from the upstream. Therefore, from these figures we can understand the structures of the secondary flow, the axial flow and the contours of the temperature distribution in duct cross-section.

3(a) 3(b)

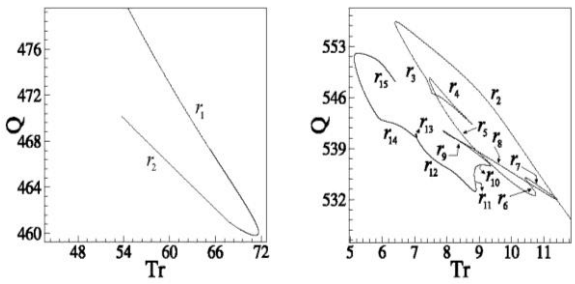

Fig 3(a)-3(b). Sections of the steady solution curve for $\gamma = 6$, $p_{gr} = 500$, $P_r = 7.0, G_r = 100$ and $5 \le T_r \le 70$.

3(c) 3(d)

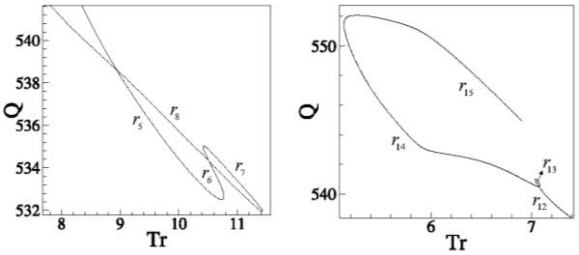

Fig 3(c)-3(d). Sections of the steady solution curve for $\gamma = 6$, $p_{gr} = 500$, $P_r = 7.0, G_r = 100$ and $5 \le T_r \le 12$.

The flow patterns and the temperature distribution are shown in Figures 4(a)-4(c) and taking four points on each section of the solution curve. We pick, $T_r = (8, 9, 10 \& 11)$ on r_5 curve, $T_r = (11, 10, 10 \& 10)$ on r_6 curve, $T_r = (5, 5, 5, 6, 6, 6, 7 \& 7)$ on r_{15} curve (eight points are taken on this curve), where the stream lines ψ, the contour plots of w and the temperature distribution T are drawn with $\Delta\psi = 1.0, \Delta w = 30.0$ and $\Delta T = 0.80$ respectively. The duct box of $\psi, w \& T$ are discussed in the previous sections. In the figures of secondary flow, solid lines $(\psi \ge 0)$ show that the secondary flow is in the counter clock-wise direction while the dotted ones $(\psi < 0)$ show that the secondary flow is in the clock-wise direction. We observed that non-symmetric solutions are obtained for $0 \le T_r \le 70$(see Figures 4(a)-4(b). As seen in Figure 4(a), the steady solution consists of asymmetric 2-vortex in the range $0 \le T_r \le 42$ on curve r_1 and strong 4-vortex with two minor vortex in the range $11 \le T_r \le 42$ on the section curves $r_1 \& r_2$, which are asymmetric with respect to $y = 0$. Also, it is seen from Figures 4(a) the secondary flow is a strong 4-vortex solution with 2 minor vortex on r_2 section curve of the solution curve generated at the outer wall of the duct. Figures 4(b)-4(c) show that the secondary flow is a strong 4-vortex

solution on the other section curves except r_1 & r_2 section curves. From these figures it is seen that the maximum axial flow is shifted to the outer wall of the duct cross-section for small values and large values of T_r. The physical mechanism responsible for such behavior is easily understood, once we recognize that the axial flow is shifted due to rotation. In figures of temperature field, the solid lines are those for $T \geq 0$ and dotted ones for $T < 0$. In Figures 4(a)-4(c), the bottom contour plots show the temperature distribution$T$. External heating sets up an intense temperature gradient at the outer wall of the duct cross-section. The contours of the temperature distribution gradually acquires strong on the outer wall, as the total flow increases or decreases. The intense of the temperature field is strong near the outer wall of the duct cross-section at strong rotational parameter associated with a large number of secondary flow vortex motion.

Plots on curve r_1 and r_2

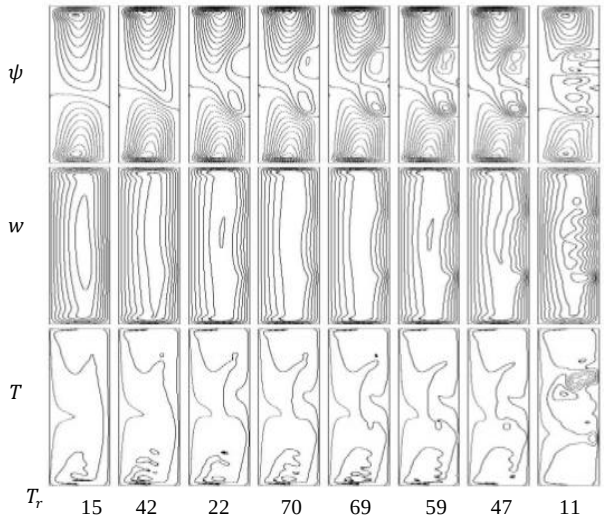

Fig 4(a). Stream lines of the secondary flow (top), Contours of the axial flow (middle) and Contours of the temperature field (bottom) of steady non-isothermal flow on r_1 and r_2 for $G_r = 100, P_r = 7.0$ and $p_{gr} = 500$ at $T_r = 15$, 42, 66, 70, 69, 59, 47 and 11 from left to right. (Actual figure size is not shown for brevity)

Plots on curve r_5 and r_6

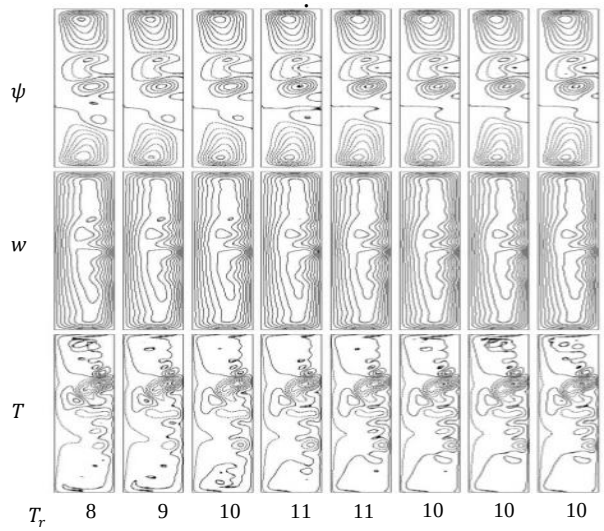

Fig 4(b). Stream lines of the secondary flow (top), Contours of the axial flow (middle) and Contours of the temperature field (bottom) of steady non-isothermal flow on r_5 and r_6 for G_r =100, P_r =7.0 and $p_{gr} = 500$ at $T_r = 8$, 9, 10, 11, 11, 10, 10 and 10 from left to right. (Actual figure size is not shown for brevity)

Plots on curve r_{15}

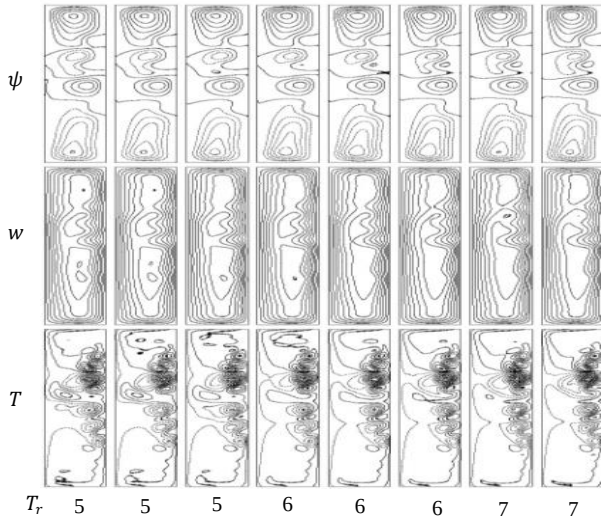

Fig 4(c). Stream lines of the secondary flow (top), Contours of the axial flow (middle) and Contours of the temperature field (bottom) of steady non-isothermal flow on r_{15} for G_r =100, P_r =7.0 and $p_{gr} = 500$at T_r =5, 5, 5, 6, 6, 6, 6 and 6 from left to right.

Case II: $\gamma = 6$ and $p_{gr} = 800$

From Figure 5, we identify 14 sections of the steady solution curve. The steady solution curve is obtained for $\gamma = 6$ and $p_{gr} = 800$ in the range $0 \leq T_r \leq 147$ and Figure 5 shows the steady solution curve. Figure 5 shows the total flow Q through the duct versus the Rotational parameter T_r. We found that at some area the sections of the steady solution curve are closed to each other (see Figure 5). The solution curve starts initially with $T_r = 0$. In the Figures 5(b)-5(d), the sections of the solution curve are shown, which are denoted by $c_1 - c_{14}$ respectively. The sections of the solution curve have increasing and decreasing behaviour as the total flow Q as well as Rotational parameter T_r increases or decreases.

The secondary flow, the axial flow and the temperature distribution at several values of T_r on the solution curve for ψ, w and T will be discussed now. The stream lines of the secondary flow, contours of the axial flow and contours of the temperature distribution are looked from the up stream of the duct cross-section.

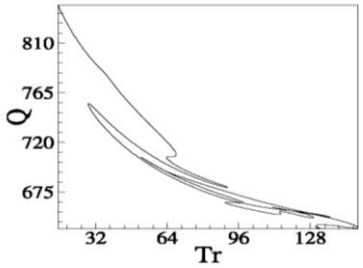

Fig 5. Steady solution curve for $\gamma = 6, p_{gr} = 800, P_r = 7.0, G_r = 100$ and $0 \leq T_r \leq 147$.

The contour plots for $\psi, w \,\&\, T$ are shown in Figures 6(a)-6(c) taking four points on each section of the solution curve. We choose, T_r = (25, 36, 47 & 57) on c_1 curve, T_r = (67, 66, 65 & 64) on c_2 curve, T_r = (117, 124, 137 & 147)

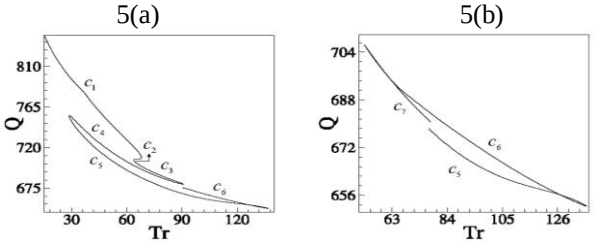

Fig 5(a)-5(b). Sections of the steady solution curve for $\gamma = 6, p_{gr} = 800, P_r = 7.0, G_r = 100$ and $18 \leq T_r \leq 138$.

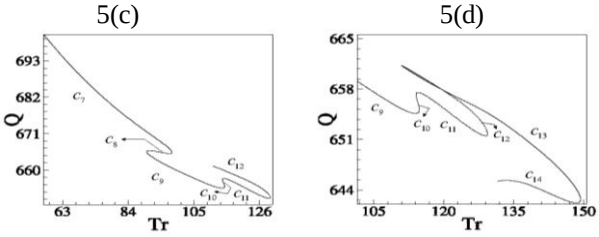

Fig 5(c)-5(d). Sections of the steady solution curve for $\gamma = 6, p_{gr} = 800, P_r = 7.0, G_r = 100$ and $52 \leq T_r \leq 147$.

on c_{11} curve, T_r = (144, 140, 137 & 132) on c_{12} curve, T_r = (130, 131, 132 & 132) on c_{13} curve, T_r = (132, 132, 131 & 131) on c_{14} curve, where the stream lines ψ, the contour plots of w and the contour plots of

Plots on curve c_1 and c_2

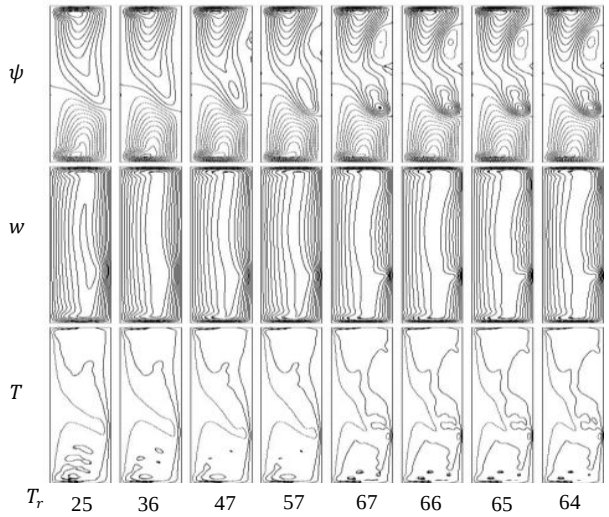

Fig6(a). Stream lines of the secondary flow (top), Contours of the axial flow (middle) and Contours of the temperature field (bottom) of steady non-isothermal flow on c_1 and c_2 for $G_r = 100, P_r = 7.0$ and p_{gr} = 800 at T_r = 25, 36, 47, 57, 67, 66, 65 and 64 from left to right.

Plots on curve c_{11} and c_{12}

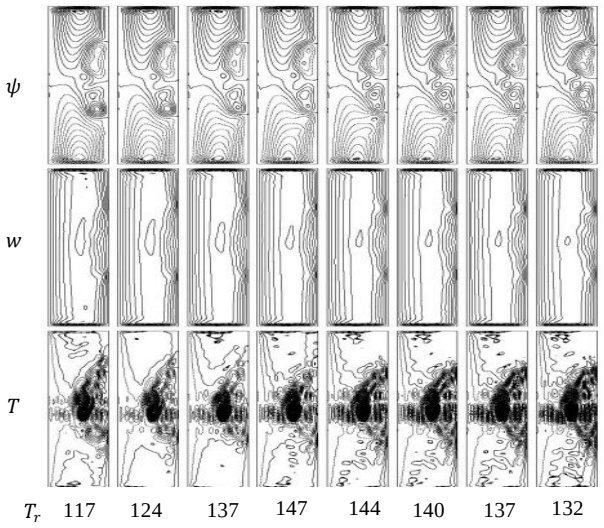

Fig 6(b). Stream lines of the secondary flow (top), Contours of the axial flow (middle) and Contours of the temperature field (bottom) of steady non-isothermal flow on c_{11} and c_{12} for $G_r = 100, P_r = 7.0$ and p_{gr} = 800 at T_r =117, 124, 137, 147, 144, 140, 137 and 132 from left to right.

Plots on c_{13} and c_{14}

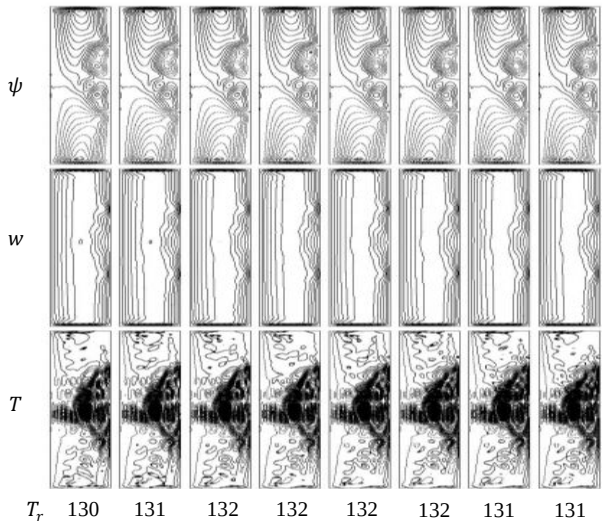

Fig 6(c). Stream lines of the secondary flow (top), Contours of the axial flow (middle) and Contours of the temperature field (bottom) of steady non-isothermal flow on c_{13} and c_{14} for $G_r = 100, P_r = 7.0$ and p_{gr} = 800 at T_r = 130, 131, 132, 132, 132, 132, 131 and 131 from left to right.

the temperature field T are drawn with the increments $\Delta\psi = 1.20, \Delta w = 35.0$ and $\Delta T = 0.50$ respectively. the secondary flow is in the clock-wise direction. We observed that, for the convective case, non-symmetric solutions are obtained for $0 \leq T_r \leq 147$ (see Figures 6(a)-6(c)). From the Figures 6(a)-6(c), it is seen that the secondary flow is :

1. 2-vortex solution on c_1 and 4-vortex solution with 2-minor vortex generated at the outer wall of the duct on c_2, c_3, c_4, c_5, c_7 and c_{10} section curves(Figure not given).
2. 6-vortex with 3-minor vortex generated at the outer wall of the duct on the section curves c_6, c_8, c_{12}, c_{13} and c_{14} of the solution curve. (Figure not given for c_6, & c_8).
3. 4-vortex solution for the first two points and 6-vortex solution for the last two points on the section curve c_{11}.

From the Figures 6(a)-6(c), we observed that the maximum axial flow is shifted from the center to the outer wall of the duct cross-section for small and large T_r. In figures of temperature field, the solid lines are those for $T \geq 0$ and dotted ones for $T < 0$. In Figures 6(a)-6(c), the bottom contour plots show the temperature distribution T. External heating sets up an intense temperature gradient at the outer wall of the duct cross-section. As the total flow increases or decreases in a certain range (see Figures 6(a)-6(c)), the contours of the temperature distribution gradually acquires strong on the outer wall. The intense of the temperature field is too high near the outer wall of the duct cross-section at large values of Rotational parameter. This type of intense is expected due to the heating of the outer wall of the duct cross-section.

5. CONCLUSIONS

According to the results, we obtained the following conclusions:

1. In both cases of large pressure-driven force (centrifugal force) and Coriolis force we obtained the multiple solutions.
2. The non-symmetric flow structures at the maximum total flow region show almost the same flow behaviour in each cases.
3. The non-symmetric 2-cell structure appears for small values of T_r and p_{gr}, while non-symmetric 6-cell structure occurs in the range of T_r (the values of T_r are large) in two cases of Rotational parameter $T_r = 100, 150$. Also the non-symmetric 10-cell structure occurs in the small range of p_{gr} (the values of p_{gr} are large) in two cases of pressure-driven parameter $p_{gr} = 500, 800$.
4. In both cases, the intense of the temperature distributions are very strong near the heated wall of the duct cross-section.

6. REFERENCES

1. G.H. Lee, J. H. Baek (2002) A numerical study of the similarity of fully developed laminar flows in orthogonally rotating rectangular ducts and stationary curved rectangular ducts of arbitrary aspect ratio, *Computational Mechanics 29*, 183-190.
2. Ito, H. (1959) Friction factors for turbulent flow in curved pipes, *Trans. ASME Journal of Basic Engineering, 81*, 123-134.
3. Ito, and Nanbu, K. (1971) Flow in rotating straight pipes of circular cross-section, *ASME Journal of Basic Engineering, September issue*, 383-394.
4. Ishigaki, H. (1994) Analogy between laminar flows in curved pipes and orthogonally rotating pipes, *Journal of Fluid Mechanics, 268*, 133-145.
5. Yang WJ, Fann S and Kim JH (1994). Heat and fluid flow inside rotating channels. *Appl. Mech. Rev. 47*, 367-396.
6. Gottlieb, D and Orszag, S.A.,(1977), Numerical analysis of Spectral Methods, *Society for Industrial and Applied Mathemetics, Philadelphia.*

7. NOMENCLATURE

Symbol	Meaning
γ	Aspect ratio
D_n	Dean Number
T_r	Taylor Number
P_{gr}	pressure deriven parameter

8. MAILING ADDRESS

Professor Dr. Md. Mahmud Alam
Mathematics Discipline
Khulna University, Khulna-9208, Bangladesh
Phone : 88-041-2831545(office)
88-041-725741 (Res.)
PABX : 88-041-721791, 720171-3,Ext.1013(Office)
Cell : 88-01912982811
FAX : 88-041-731244
E-mail : alam_mahmud2000@yahoo.com
joy_math00@yahoo.com
Web : www.math.ku.ac.bd